ULTRASONIC PROPAGATION IN MOLTEN LITHIUM-, SODIUM-, AND POTASSIUM-SILICATES

Yutaka Shiraishi
AGNE Gijutsu Center Inc., Japan

Masaki Yamashita, Yuichiro Tokunaga, Atsushi Tanaka,
Tohru Kanno & Katsutoshi Takano
Tohoku University, Japan

ABSTRACT

Velocity and attenuation of ultrasonic wave in molten alkaline silicates of lithium, sodium, and potassium were measured at a temperature range between their liquidus and about 200K higher than liquidus. Measurements were carried out by the pulse transmission method using a couple of ultrasonic pulse generator and receiver. Composition of the silicate sample was selected as enough temperature range was obtained and to get the correct knowledge of composition dependence on silicate. Measured velocity of ultrasound decreases with the increase of temperature in all samples. Composition dependence were similar between sodium and potassium silicates but little different in lithium silicate. Absorption of ultrasound depends both on the sound frequencies and temperatures. It suggests there is some dispersion of sound waves propagating in the silicate medium. Since the lithium silicate melt behaves in a dissimilar way from those of other alkaline silicates, we tried the additional measurement on the pseudo-binary system of lithium disilicate and sodium disilicate system. The results are discussed from the structural aspect comparing with the previous work on Ni ion color indicator.

INTRODUCTION

Ultrasonic wave is characterized by its high directionality and strong accelerative field. These properties are utilized for many fields of industry. For example, high directionality can be applied to measure the distance through an opaque medium instead of light. A typical example may be sonar. For example, strong acceleration of the ultrasonic wave can be applied to the washing of a materials and dispersion of the fine particle into a medium. The acceleration of medium α, is expressed for the medium displacement ξ, as; $\alpha = (2\pi f)2\xi$. Thus the acceleration is about 10^6 times as large as the acceleration of gravity for 1μm displacement at 1MHz oscillation. Such strong acceleration in the medium causes the cavity in it. Shock wave generating from vanishing of the cavity gives a very strong force and is utilized many purposes, such as making an emulsion. These characteristics should be applied to high temperature processes. Some applicative trials have been made on continuous casting. Ultrasonic is irradiated into the freezing ingot to minimize the surface and inner defect of the ingot [4]. The idea of utilizing cavitation to eliminate a gas and inclusion from the bulk melt was tested in a cold model experiment [3]. Many new ideas are proposed. But many difficulties impede the realization of such ideas and wait to be solved in future.

Fundamental knowledge on the ultrasonic properties of melt is useful for industrial application. Apart from such practical purposes, investigation on the ultrasonic properties of the melt is important for the understanding of molecular structure of matter and the relaxation behavior of molecular motion. From such point of view, some studies have been reported on the ultrasonic propagation through the molten slag [5] and silicates [7].

EXPERIMENT

Method of Measurement

Pulse transmission method is used both velocity and absorption measurements. Block diagram of measuring circuit is shown in Figure 1. Most of the circuit units are utilized by Matec's product, *Ultrasonic attenuation and velocity measurement assembly* as shown in Figure 1.

Ultrasonic velocity is measured from the delay time and the traveling distance of the sound pulse through the sample melt. Gradient of the delay time plotted against the traveling distance gives a sound velocity. Since the absolute value of traveling distance of sound can not be determined easily, we use relative measurement both for distance and delay time. When the relative delay time, Δt, is measured against the traveling distance, Δx, the regression value of the slope gives the ultrasonic velocity, u, in the medium.

$$u = \Delta x / \Delta t \tag{1}$$

Delay time is measured by an echo-superimpose method. Namely, the first peak of received wave is overlapped to the started peak by the operation of the dual delay generator, (Model 122B) and necessary time is read out from the frequency counter.

Absorption coefficient of the ultrasonic wave is determined by automatic attenuation recorder, (Model 2470A). Received wave height is compared with the reference height in the attenuator and its attenuated value is given in a decibel scale. Thus, the absorption coefficient, α' is given by the equation;

$$\alpha' = \Delta \log(I/I_0)/\Delta x = \Delta \mathrm{dB}/\Delta \tag{2}$$

where, I_0 and I are peak height at reference position and at x, respectively.

Attenuation coefficient is usually expressed by the unit, neper/m; as an amount of attenuation per m described in natural logarithm. Relation with Equation 2 is

$$\alpha\ [\text{neper/m}] = \alpha'\ [\text{dB/m}]/8.686 \tag{3}$$

Experimental Apparatus

High temperature part of the experimental apparatus is schematically shown in Figure 2. Electrical pulse is introduced to the upper oscillator, X-cut quartz, and converted to mechanical vibration, *i.e.* ultrasonic pulse. Generated pulse by quartz oscillator is conducted through a sapphire rod having 15 mm diameter and 320 mm long, into the molten sample which is contained in the platinum crucible. Ultrasonic pulse passed through the sample melt is conducted by a sapphire rod having 20 mm diameter and 250 mm long, to the bottom oscillator, X-cut quartz and converted to the electrical pulse. The platinum crucible having 40 mm diameter is supported by lower sapphire rod with ground fitting. All the oscillator crystals are fixed on the polished end of sapphire rods with phenyl salicylate paste. For the protection from the heat, sapphire rods are cooled by water.

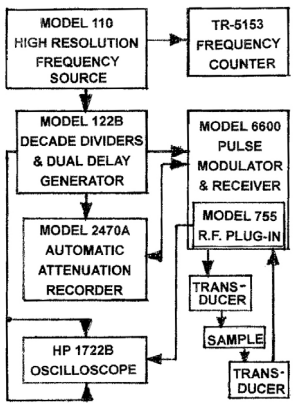

Figure 1: Block diagram of measuring circuit

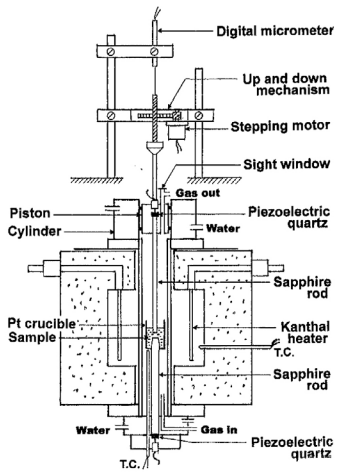

Figure 2: Experimental apparatus for the measurement of ultrasonic propagation in molten silicates

Upper sapphire rod is required a precise motion in a vertical direction. For this purpose, the rod is fixed to the piston moving smoothly in the cylinder and is driven by a stepping motor through a mechanism of gear and screw. Traveling distance is measured by a digital micrometer in ±1 μm precision.

The furnace has six super kanthal heater rods arranged in radial direction. Temperature of the sample melt is measured by Pt/Pt·13%Rh thermocouple located underneath of the platinum crucible. Atmosphere surrounding the sample is kept inert by dry argon stream throughout the measurement.

Procedure of the measurement is as follows: Both sapphire rods pasted the oscillating crystal on one end are fixed to their right position. Namely, upper rod is fixed to the piston and lower rod is fixed to the bottom flange. At first, confirmation has been done

for getting enough strength of the reflection signal by echo method on each rod. The crucible is then filled with the sample powder up to about 3/4 in volume, and argon gas is introduced to the furnace. Following the thorough replacement by argon gas, the sample is heated up to melt. At the desired temperature, upper sapphire rod is dipped to the melt and the ultrasonic pulse is conducted into the sample melt. Measurements were generally carried out in an ascending temperature and all the procedure were repeated twice at a minimum. Velocity and absorption measurement were made separately at the desired temperature and source frequency is changed after a sequence of velocity or absorption measurement. After measurement were done, sample melt were then sucked out from the crucible by opaque quartz tube to prevent the deformation of the crucible and damage of the sapphire rod as possible. Traveling distance of the upper rod is one millimeter or less and total gap between two rods is less than two millimeters.

Samples are prepared from the reagent grade of silica and alkaline metal carbonates. They are weighed in desired amount then mixed well and fused in a platinum crucible. After thorough mixing in molten state, melt is poured out onto a stainless steel plate. Cooled glass of the sample is crushed into granular powder and served for measurements.

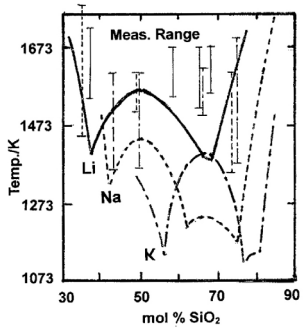

Figure 3: Liquids lines of alkaline silictaes and measured composition and temperature range

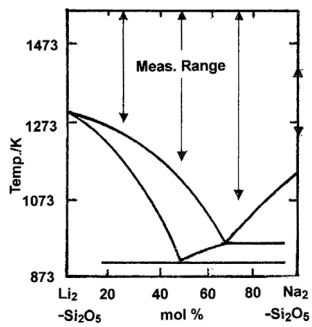

Figure 4: Liquids line of pseudo-binary system of Li and Na disilicate with composition and temperature range of the samples

Composition is determined by analysis for several samples. Since no significant difference was observed between analyzed and nominal composition, then we use the nominal value throughout the experiment as a sample composition.

Composition and the temperature range for measurement are given in Figures 3 and 4. Figure 3 shows the liquidus lines of lithium, sodium, and potassium silicate systems. Vertical bar means the composition and the temperature range for each measurement. Figure 4 is also shown the phase diagram of pseudo-binary system of lithium and sodium disilicate with measured composition and temperature range.

RESULTS

Since the rod shape transducer is used in this experiment, sound wave is reflected on the wall of the transducer and some times, trailing pulses follow after the main pulse. This effect becomes significant at a lower frequency and gives a distortion of the pulse shape. Thus we select the frequency range as five to fifteen MHz. This lower frequency fulfilled avoiding the Fresnel region [10], in which the lower limit of frequency is calculated as about five MHz from the geometry and sound velocity of the sapphire. The upper limit of frequency is determined from the observable strength of the transmitted pulse, as the higher frequency pulse attenuates quickly.

Results are summarized in Table 1, 2, 3 and 4. All figures given in the tables are interpolated value to specified temperatures given in the column. Experimental values are shown as plotted points in Figure 5, for example. Sound velocity decrease with temperature in all systems.

Comparisons with other available data are also given in Figure 5. There are some discrepancies at lower temperatures but discrepancies become smaller at higher temperatures. The origin of discrepancy is not clear. The effect of frequency on the velocity can not be observed in most cases except the pseudo-binary system of $Li_2Si_2O_5$ - $Na_2Si_2O_5$ as shown in Table 1 and 2. Figures 7 and 8 show the velocity vs. composition relationships in alkaline silicates and in disilicate system of lithium and sodium, respectively. In Figure 8, two kinds of curves are shown, one is the ordinary isothermal data and the other indicates the data along 200 K higher than the liquidus. Undulation at 1450 K isotherm disappeared liquidus plus 200 K curve.

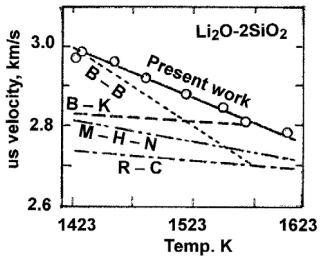

Figure 5: Ultrasonic velocity vs. temperature Li_2O-$2SiO_2$ melt. [1], B-K: Baidov and Kunin, [6, 7]

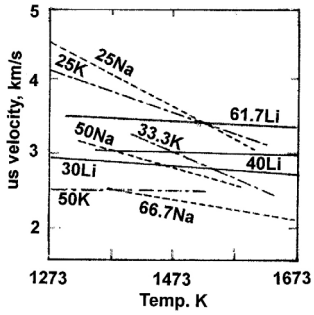

Figure 6: Ultrasonic velocity vs. temperature relationship in alkaline silicates. Atached numbers and symbol shows mole % of the corresponding oxide

Probably, this kind of undulation is attributed to the effect of temperature difference between isotherm and liquidus, which vary with composition.

Table 1: Ultrasonic velocity u(m/s) and compressibility, $\beta \times 10^{-11}$ in molten alkaline silicates

Data by interpolation

System: mol% R_2O - SiO_2

	u at Temp./K				β/m²/N		u at Temp./K					β/m²/N
T =	1423	1473	1573	1623	1473K	T =	1273	1373	1473	1573	1673	1473K
Li_2O mol %, f = 7~11 MHz						**Na_2O mol%,** f = 5~20 MHz						
30	3000	2920	2760		5.42	25	4550	4090	3650	3200		3.34
33	3020	2960	2840		5.57	50			2790	2550		5.71
40	3220	3200	2970		4.51	66.7			2340	2190	2090	
61.7	3640	3580	3480	3430								
						K_2O mol%, f = 10 MHz						
						25	4140	3880	3610	3340	3080	3.47
						33.3	3230/1423K	3070	2750		4.81	
						50	2560	2510	2460	2240/1523K		
						56.4	2390	2330	2260	2230/1523K		

Tables 3 and 4 show the attenuation coefficient α in dB/mm. Classical expression of the quotient of absorption coefficient and frequency, α/f^2 does not depend to frequency as shown in Equation 5. In this study, however, all values of α/f^2 depend on the frequency, but also depend on temperature, as shown in Figure 9.

This effect is more remarkable in acid region of the system and make a maximum around 1400~1500 K in Na- and K-silicates, but non in Li-silicate system. To make clear the behavior of lithium ion, absorption measurement is also carried in pseudo-binary system of Li-Na-disilicate. In these melts, absorption maximum are also observed in Na-rich composition at a little lower temperatures of 1200~1300 K.

Adiabatic compressibility is calculated from ultrasonic velocity combining with available density data [7] and is given in the Tables 1.

Table 2: Ultrasonic velocity u(m/s) in molten pseudo-binary system of $Li_2Si_2O_5$-$Na_2Si_2O_5$. Data by interpolation

	u /m/s at Temp. / K							**u /m/s at Temp. / K**				
T =	1073	1173	1273	1373	1473	1573K	T =	1173	1273	1373	1473	1573K
$Na_2O•2SiO_2$							**$Li_2O•2SiO_2$ - $Na_2O•2SiO_2$**					
f = 6 MHz		3940	3780	3390	(3000)		f = 7.1 MHz	3745	3525	3305	3085	3865
10		4050	3860	3370	(2880)		11.5	4080	3820	3400	3100	2740
15.3		4210	3920	3200	(2470)							
$Li_2O•2SiO_2$ - 3($Na_2O•2SiO_2$)							**3($Li_2O•2SiO_2$) - $Na_2O•2SiO_2$**					
f = 6.5 MHz	3940	3750	3615	3450	3290	3130	f = 6.7 MHz		3330	3310	3300	3280
11.3	4900	4510	4150	3780	3400	3030	11.2		3600	3555	3430	2280
16.2	5130	4780	4430	4080	3930	3380	14.6		4170	4005	3840	3680

Table 3: Attenuation coefficient a /dB/mm of ultrasonic wave in molten alkaline silicates. Data by interpolation

System\T	**a/dB/mm at Temp./K**					**System\T**	**a/dB/mm at Temp./K**				
40 Li_2O-60 SiO_2	**1273**	**1373**	**1473**	**1573 K**		**33.3 Na_2O-66.7 SiO_2**	**1273**	**1373**	**1473**	**1573 K**	
7.1 MHz		7.672	2.380			14.28	20.01	21.56	21.47		
11.6			5.484	2.868							
33.4 Li_2O-66.6 SiO_2		**1423**	**1473**	**1573 K**		**25 Na_2O-75 SiO_2**	**1273**	**1373**	**1473**	**1573**	**1673 K**
7.0 MHz		14.83	7.64	2.76		5.78 MHz	13.54	28.39	29.98	15.18	
11.7		18.41	13.16	5.75		14.0	15.82	33.18	44.52	35.80	9.20
30 Li_2O-70 SiO_2		**1423**	**1473**	**1573K**		**56.4 K_2O-43.6SiO_2**	**1273**	**1373**	**1473**	**1573 K**	
7.1 MHz		23.13	11.82	4.44		6.3 MHz	1.37	2.74	3.50	(5.62)	
11.6		30.48	22.26	10.61		11.4	3.50	4.60	5.73	(16.9)	
56.4 Na_2O-43.6 SiO_2			**1533**	**1573**	**1623 K**	**50 K_2O-50 SiO_2**	**1273**	**1373**	**1473**	**1573 K**	
5.62 MHz			8.23	1.77		6.3 MHz	3.98	5.15	7.40		
14.65				0.60	0.23	11.5		4.69	5.92	8.00	10.97
50 Na_2O-50 SiO_2		**1423**	**1473**	**1573**	**1623 K**	**33.3 K_2O-66.7 SiO_2**		**1373**	**1473**	**1573**	**1673 K**
5.74 MHz		0.48	0.36	0.25	0.23	6.3 MHz		9.95	21.61	23.84	
14.24		1.92	1.47	1.02		11.5		1.47	20.57	29.14	18.86
33.3 Na_2O-66.7 SiO_2	**1273**	**1373**	**1473**	**1573 K**		**25 K_2O-75 SiO_2**	**1273**	**1373**	**1473**	**1573**	**1673 K**
5.52 MHz	16.50	23.75	10.06	5.85		5.9 MHz	4.19	9.73	20.35	40.70	28.44
						11.5	7.39	16.50	26.73	39.24	35.27

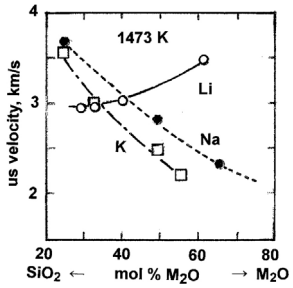

Figure 7: Velocity vs. mole% of alkaline oxides at 1473 K. f=5-15 MHz

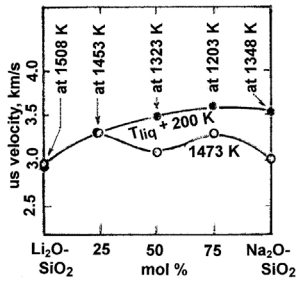

Figure 8: Velocity in pseudo-binary system of Li and na disilicates

Table 4: Attenuation coefficient in molten pseudo-binary system of $Li_2Si_2O_5$ - $Na_2Si_2O_5$. Data by interpolation

System\T	α/dB/mm at Temp. K						System\T	α/dB/mm at Temp. K				
$Na_2Si_2O_5$		**1233**	**1273**	**1323**	**1373**	**1413 K**	**($Na_2Si_2O_5$) - (Li_2SiO_5)**	**1173**	**1273**	**1373**	**1473**	**1573 K**
f = 10.7 MHz		10.48	19.20	28.03	29.00	20.35	f = 7.09 MHz	13.38	14.97	10.08	4.03	1.74
15.3		14.20	20.35	29.56	32.83	25.15		11.49	12.66	21.59	14.11	9.00
3.47												
3($Na_2Si_2O_5$) - Li_2SiO_5	**1073**	**1173**	**1273**	**1373**	**1473**	**1573 K**	**$Na_2Si_2O_5$ -3(Li_2SiO_5)**		1273	1373	1473	1573 K
f = 6.46 MHz	8.44	16.65	16.88	13.03	7.96		f = 6.75 MHz		12.40	9.21	6.71	3.84
11.28	9.65	20.41	24.13	13.17	17.86	7.72						
16.14	11.24	24.60	30.88	32.82	30.40	24.36	11.19		31.10	24.95	11.52	4.60

DISCUSSION

Our discussion will center around the maximum absorption curve shown in Figure 9 and the exception of the lithium oxide system.

Beside the theoretical argument, well known formulae on velocity u and absorption coefficient α of sound propagating through an homogeneous and isotropic medium, like a liquid, can be expressed as:

$$u = (K/\rho)^{1/2} = (1/\beta\rho)^{1/2} \quad (4)$$

and

$$\alpha = (2\pi f^2/\rho u^3)(\eta_b + \eta_s) \quad (5)$$

where, K is the volume elasticity, β is the adiabatic compressibility, f is the frequency, and η_b, η_s are volume and shear viscosity coefficients, respectively. In these equations, the assumption that $\alpha u/2\pi f << 1$, and volume elasticity is much larger than shear elasticity, is usually fulfilled for the liquid. These equations indicate that the velocity and the quantity α/f^2 are independent of the sound frequency. If these quantities depend on the frequency, then we expect some relaxation phenomenon to happen during the propagation process of sound.

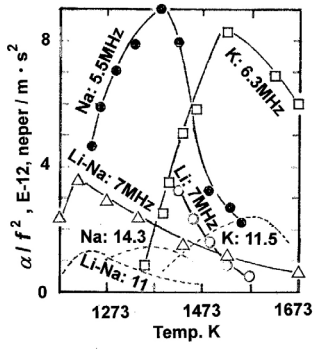

Figure 9: Attenuation coefficient vs. temperature in alkaline disilicate systems. Attached symbols show the kind of oxide and measuring.

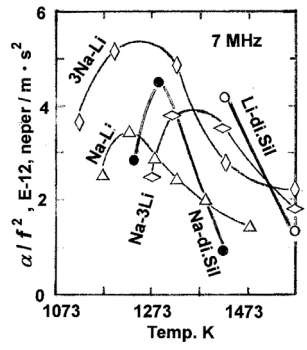

Figure 10: Attenuation coefficient vs. temperature in pseudo-binary system of Li and Na disilicates. Attached number indicates mole ratio of each disilicate.

Available data, by Zuh *et al.* (1994), in which the velocity and the absorption of ultrasonic propagation are measured precisely on molten alkaline halides, nitrates, and carbonates, reported no effect of frequencies over the range 5~85 MHz. On the contrary, our data are strongly indicate the affect of the frequency, especially in absorption measurements.

In general, the *extra-effect* of frequency is attributed to the relaxation effect of the internal freedom, such as molecular vibration, molecular rotation, and chemical reaction and so on. Form such point of view, we must consider what kind of relaxation may take place in the silica rich composition of sodium and potassium silicate melts, and does not take place in the lithium silicate.

Though an exact treatment of such relaxation phenomenon is available [10], a more intuitional way is adopted here. Under the assumption, $\eta_b >> \eta_s$, Equation 5 is rewritten as;

$$(\alpha/f^2)(\rho u^3/2\pi) = \eta_b \tag{6}$$

Here, we assume the thermal activation process and apply Arrhenius type formalism. Then,

$$(\alpha/f^2)(\rho u^3/2\pi) = \eta_b^0 \exp(E_{\eta b}/RT) \tag{7}$$

where, $E_{\eta b}$ is the activation energy of bulk viscosity.

If Equation 7 is this case, apparent activation energy can be determined as a slope of $\ln[(\alpha/f^2)\ (\rho u^3/2\pi)]$ vs. $(1/T)$ plot. By this method, we obtained the apparent activation energy as Figure 11. Average value is scattered around 30 kJ/mol, for both sodium and potassium disilicate melts.

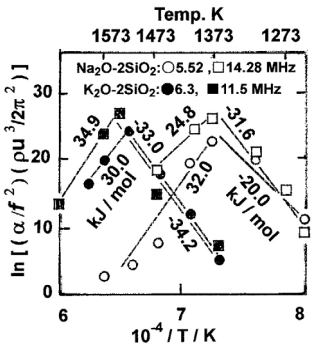

Figure 11: Apparent activation energy of the bulk viscosity in Na and K disilicate

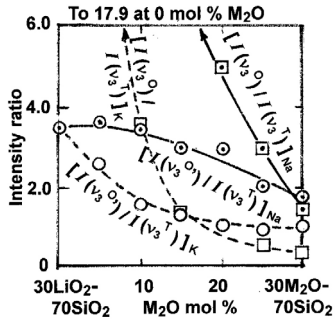

Figure 12: Relative intensity of absorption band due to Ni^{2+} coordinated to an oxygen as octahedral; v° or tetrahedral; v^{T} in $(30\text{-}x)Li_2O\text{-}xR_2O\text{-}SiO_2$ glass. R= Na or K

The sign of the activation energy is opposite on both sides of the temperature corresponding to maximum absorption. If the relaxation mechanism is the same on both side of temperatures, absolute value of the activation energy must be the same. This condition is fulfilled in this experiment. We thus concluded the same mechanism is held on both sides of activation and deactivation processes.

The same order of the magnitude of activation energy is obtained for the absorption process in Na and K silicate system. Those values are nearly the half of those in self-diffusion of alkaline metal ions in disilicate melt, Nagata (1988), which are reported as roughly 50 kJ/mol. This fact means the relaxation process in ultrasonic absorption can occur easier than the self-diffusion process. So, the freedom of translational motion is excluded from the relaxation process in ultrasonic propagation. From the magnitude of the activation energy, we must consider a rotational or rotational vibrational mode as a possible relaxation process.

Other information comes from molecular dynamic simulation of silica structure. Soules reported the relaxation behavior of silicon-oxygen bonding in silica glass at 1500 K [9]. He showed that the four fold and three fold oxygen atoms coordinated to silicon atom needed a rather lengthy time for relaxing compared with the bridging or non-bridging oxygen atom. This implies that the rotational motion of bridging or non-bridging oxygen can take place easily than that of four or three coordinated oxygen atoms.

As shown above, lithium oxide behaves as singular manner in silicate melt compared with the other alkaline oxides such as sodium or potassium oxide. The origin of this difference should be come from the strong ionic strength of lithium ion. Ionic radius of lithium ion is 0.060 nm and comparable with the radii of Fe^{3+}(0.060) and V^{4+}(0.061). It is possible to coordinate lithium ion with 4 or 6 oxygen atoms. Then, Li^{+} can occupy not only the octahedral interstice of oxygen but also tetrahedral interstice. This is a big difference among the other alkaline metal oxides and implies the possibility of substitution for the network forming ion though such network can not be stable.

In our previous work [8] on optical absorption spectrum of Ni^{2+} ion in alkaline silicate glasses, we concluded that Ni^{2+} ion takes preferentially the 4-coordinated octahedral arrangement rather than 6-coordinated octahedral arrangement in sodium and especially in potassium silicate. This conclusion means the tetrahedral site in silicate network becomes vacant when Li^{+} ion replaces by Na^{+} or K^{+} ion, namely, the network becomes an open structure by the substitution of Na^{+} or K^{+} ion for Li^{+} ion.

This means Li^{+} ion can make a pseudo-network in a short time scale though ionic charge is not enough to keep a stable network. It may, however be enough to prevent the rotational motion which takes place in the sodium or potassium silicate to melt.

CONCLUSIONS

Ultrasonic velocity and absorption in molten alkaline silicates were measured. With alkaline oxide, lithium oxide behaves in a peculiar manner compared with other alkaline oxides. Some discussion is given on the relaxation phenomena appeared in ultrasonic absorption with special attention to the behavior of lithium oxide.

REFERENCES

Bloom, H. & Bockris, J. O'M. (1957). *The Compressibility of the Silicate: The Li_2O-SiO_2 System.* J. P. C. 61, pp. 515-518. [1]

Bockris, J. O'M. & Kojonen, E. (1960). *The Compressibility of Certain Molten Alkali Silicates and Borates.* J. P. C. 85, pp. 4493-4497. [2]

Kuwabara, M. (2007). *New Rends of Sonoprocessing of Materials in Liquid State.* CAMP- ISIJ, 20, pp. 720-723. [3]

Yasuda, K., Yang, J., Liu, Z. & Kuwabara, M. (2007). *The Effect of Acoustic Cavitation on Solidified Structure of Metal Alloy.* CAMP-ISIJ, 20, pp. 729-734. [4]

Matsushita, T., Hayashi, M. & Seetharaman, S. (2005). *Thermochemical and Thermo-Physical Property Measurements in Slag Systems.* Int. J. Materials and Product Technol., 22, pp. 351-390. [5]

Matsuzono, Y., Hayashi, M. & Nagta, K. (2007). *Accurate Measurement of the Velocity and Absorption of Molten Alkali Silicates.* CAMP-ISIJ, 20, p. 126 (Jap). [6]

Rivers, M. L. & Carmichael, S. E. (1987). *Ultrasonic Studies of Silicate Melts.* J. Geophy. Research, 92, B9, pp. 9247-9270. [7]

Shiraishi, Y. & Iwakura, M. (1992). *Optical Absorption Spectrum of Ni^{2+} Ion in Alkaline Silicate Glasses.* Bull. Inst. Adv. Matr. Processing, Tohoku Univ. 48, pp. 19-29 (Jap). [8]

Soules, T. F. (1990). *Structural Relaxation in Silica Melt.* J. Non-Cryst. Solids, 123, p. 48. [9]

US Hand Book. (1999). Ultrasonic Hand Book, Ed. Hd. Bk. Comm., (Chair.Takagi), Pub. Maruzen, Tokyo, pp. 243-246 (Jap). [10]